

# New methodology for the determination of hydrogen permeation parameters in layered materials

P. E. V. DE MIRANDA, F. D. FASSINI

*EE-COPPE, Federal University of Rio de Janeiro, P.O. Box 68505, 21945. 970 Rio de Janeiro, RJ, Brazil*

A new methodology for interpreting hydrogen permeation test data has been proposed with the objective of determining hydrogen permeability, solubility and diffusivity in materials containing surface-coating layers. The mathematical development of equations has been undertaken for steady-state hydrogen permeation conditions allowing the determination of all parameters of interest for the composite material and the coating layer itself. For a single-layered material, a set of three statistically significant permeation tests is enough to determine all variables for the substrate, the composite material and the coating layer. This methodology has been applied to published results on the hydrogen permeation in nitrogen ion-implanted extra-low carbon steel, showing that the hydrogen diffusion coefficient in such a coating layer is several orders of magnitude lower than that in the substrate. The hydrogen solubility in the layer is, by contrast, increased. The magnitudes of these effects depend on the nitrogen concentration in the surface layer.

## 1. Introduction

Since the early works performed by Devanathan and Stachurski [1] and by Boes and Züchner [2] on the electrochemical methods for the determination of the kinetics of hydrogen permeation in materials, a wide variety of research work has been carried out using such procedures. The relative simplicity and well-established practice for conducting laboratory electrochemical experiments, as well as the availability of mathematical descriptions of the physical phenomena involved therein, has facilitated the determination of hydrogen permeability, solubility and, especially, diffusivity in pure metals [3], steels [4] and amorphous materials [5], among others. An important requirement for employing such methodologies was the use of samples structurally homogeneous throughout their thicknesses. That is, in principle, approximately the same overall distribution of atom species and particles should be present throughout the diffusion path of hydrogen in the material for the boundary conditions to Fick's second law differential equation to be properly taken into account. This ruled out the possibility of using the same routine of analysis as for electrochemical permeation tests data, as previously mentioned for layered materials, for the simple reason that these act as composite materials, for which the hydrogen permeation kinetics of the layer may be indeed considerably different from that of the substrate. To cite a few examples, this is the situation actually occurring when a low-alloy structural steel is clad with an austenitic steel, when a metal or alloy is coated with an enamel, with ceramic layers obtained by sol-gel processes or others, or when amorphous

surface layers are produced by laser or ion-implantation techniques.

The interest in developing coatings to act as impeding layers for the penetration of hydrogen into materials, with the purpose of limiting hydrogen embrittlement of components, motivated the present work, which aimed to describe a new methodology, using electrochemical permeation tests, which enables hydrogen permeability, solubility and diffusivity in layered materials to be determined. This has the further special advantage of furnishing these parameters for the bulk composite material, as well as for the coating layer itself.

## 2. Conventional methodology for non-layered materials

The various electrochemical techniques available for the determination of hydrogen permeation in materials make use of a double electrolytic cell, in which the sample is interposed between two compartments. Each of these represents a three-electrode electrolytic cell, these electrodes being the sample as the working electrode, a reference electrode (such as a saturated calomel electrode), and a counter electrode of a noble metal, such as platinum. Each cell contains a deaerated electrolyte (such as 0.1 N NaOH) thermostatically controlled at the desired temperature. Hydrogen is generated in one of the compartments to be adsorbed at the surface of, and absorbed by, the sample, penetrating by solid-state diffusion throughout its thickness,  $l$ , until it reaches the opposite face of the sample and is detected in the other compartment

of the electrochemical cell. The technique chosen for the present study is characterized by a cathodic potentiostatic polarization on the hydrogen generation side and by an anodic polarization at the hydrogen detection side of the cell. This was called the non-steady-state potentiostatic time-lag method by Boes and Züchner [2] and here will be simply termed the double-potentiostatic technique.

Holding the electrolytic cell of the hydrogen detection compartment under anodic polarization throughout the test, while a cathodic polarization is performed in the hydrogen generation compartment, ensures the oxidation of the hydrogen atoms that reach the electrolyte, on leaving the sample. As a result of that, the hydrogen concentration at the surface of the sample facing the detection compartment is kept at zero and an electric current,  $I_1(t)$ , flows, and builds up with time, between the sample and the counter-electrode. This current eventually reaches a steady state value,  $I_\infty$ , when a steep hydrogen concentration gradient is established through the sample thickness, varying linearly from the hydrogen solubility limit,  $S$ , at the surface of the sample facing the hydrogen generation compartment, to zero, at the sample's surface facing the hydrogen detection compartment. Taking the limits of this hydrogen concentration gradient as the boundary conditions, and assuming that the sample was originally free of hydrogen, as the initial condition, Fick's second law differential equation may be solved as a function of the position along the sample's thickness ( $0 \leq x \leq l$ ) and time,  $t$ , for a sheet-type sample for which unidirectional solid-state diffusion predominates. By differentiating this solution with respect to time at  $x = l$  and applying Faraday's law, one obtains an equation describing the variation of the anodic current with time,  $I_1(t)$ , from which the hydrogen diffusion coefficient,  $D$ , may be readily determined [1, 2]. This anodic current,  $I_1(t)$ , is proportional to the flux of hydrogen,  $F$ , permeating the sample and, for long times (as  $t \rightarrow \infty$ ,  $I_1(t) \rightarrow I_\infty$ ,  $F(t) \rightarrow F_\infty$ ), it defines the steady-state hydrogen permeability throughout the material,  $P_\infty$ , by

$$P_\infty = F_\infty l = DS \quad (1)$$

from which the hydrogen solubility in the sample,  $S$ , may be obtained.

### 3. New methodology for the determination of hydrogen permeation parameters in layered materials

Consider a multilayered sheet sample, containing  $n$  different coating layers, with which a double-potentiostatic hydrogen permeation test is conducted at constant temperature. When a steady state is reached, that is, when  $I_1(t)$  is equal to  $I_\infty$ , the flux,  $F$ , of hydrogen through the  $i$ th layer is the same through any other, as well as for the whole sample thickness, and may be simply expressed by Ficks' first law for unidirectional solid-state diffusion as

$$F = -D_i \frac{\partial C}{\partial x} \quad (2)$$

where  $C$  is the hydrogen concentration. If  $D_i$  is independent of concentration, showing no variation with position within a layer, and if there are no diffusion barriers at the interfaces between the layers, integration of Equation 2 with respect to  $x$  gives

$$F = \frac{D_i \Delta C_i}{x_i - x_{i-1}} \quad (3)$$

where  $D_i$  and  $\Delta C_i$  are, respectively, the hydrogen diffusion coefficient for and the range of hydrogen concentration through the  $i$ th layer.

The steady-state hydrogen flux,  $F_\infty$ , through the whole sample's thickness will be

$$F_\infty = \frac{\bar{D} \Delta C}{l} \quad (4)$$

where  $\bar{D}$  is the effective hydrogen diffusion coefficient for the composite material, and  $\Delta C$  is the total hydrogen concentration range through the sample, taken as

$$\Delta C = \Delta C_1 + \Delta C_2 + \dots + \Delta C_i + \dots + \Delta C_n \quad (5)$$

Equation 4 may be re-written as

$$F_\infty = \frac{\bar{D}}{l} (\Delta C_1 + \Delta C_2 + \dots + \Delta C_i + \dots + \Delta C_n) \quad (6)$$

for which

$$\begin{aligned} \Delta C_1 &= \frac{F_1 l_1}{D_1}, \Delta C_2 = \frac{F_2 l_2}{D_2}, \dots, \\ \Delta C_i &= \frac{F_i l_i}{D_i}, \dots, \Delta C_n = \frac{F_n l_n}{D_n} \end{aligned} \quad (7)$$

$F_1, F_2, \dots, F_i, \dots, F_n; D_1, D_2, \dots, D_i, \dots, D_n$  and  $l_1, l_2, \dots, l_i, \dots, l_n$  are, respectively, the hydrogen fluxes through, the diffusion coefficients for, and the thicknesses of the different layers.

Because at steady state  $F_\infty = F_1 = F_2 = \dots = F_i = \dots = F_n$ , it follows that

$$\frac{1}{\bar{D}} = \frac{l_1}{D_1} + \frac{l_2}{D_2} + \dots + \frac{l_i}{D_i} + \dots + \frac{l_n}{D_n} \quad (8)$$

Equation 8 is a consequence of the fact that at steady state the total drop of hydrogen concentration through the whole sample's thickness for a multi-layered sample composed of  $n$  different layers with thicknesses  $l_1, l_2, \dots, l_i, \dots, l_n$  and hydrogen diffusion coefficients  $D_1, D_2, \dots, D_i, \dots, D_n$  is equal to the sum of the hydrogen concentration drops through each individual layer [6].

For the simple case of a sheet substrate containing only one coating layer on one of its faces, the methodology for the determination of hydrogen permeation parameters is composed of three steps.

#### 3.1. Step one: permeation through the substrate

This step consists of conducting a conventional

double-potentiostatic hydrogen permeation test on the substrate, with thickness  $l_s$ . With this experiment the steady-state hydrogen permeability,  $P_{\infty s}$ , will be measured, the hydrogen diffusion coefficient,  $D_s$ , will be determined as usual [1, 2] and the hydrogen solubility,  $S_s$ , will be calculated by using the relation

$$S_s = \frac{P_{\infty s}}{D_s} \quad (9)$$

### 3.2. Step two: permeation from the substrate to the coating layer

This consists of conducting a double-potentiostatic hydrogen permeation test with a coated sheet sample of total thickness equal to  $l$  and coating thickness equal to  $l_c$  positioned in such a way that the uncoated (substrate) surface of this sample faces the hydrogen generation compartment of the double-electrolytic cell and, hence, the coating layer faces the hydrogen detection compartment. This test configuration permits the elimination of one, as yet unknown variable, the hydrogen solubility in the coating layer,  $S_c$ , because the surface of the sample facing the hydrogen detection compartment of the double-electrolytic cell will be forced, as required by this type of hydrogen permeation test, to have a hydrogen concentration equal to zero.

The effective hydrogen permeability,  $\bar{P}_{\infty sc}$ , for the permeation being conducted from the substrate to the coating, may be obtained from the experimentally measured value of the anodic (detection) current at the steady state in such tests, from which the effective hydrogen diffusion coefficient,  $\bar{D}$ , may be determined at steady state by

$$\bar{D} = \frac{\bar{P}_{\infty sc}}{S_s} \quad (10)$$

Finally, applying Relation 8 to the present case, for which  $l = l_s + l_c$ , the hydrogen diffusion coefficient for the coating layer,  $D_c$ , may be calculated (provided  $l_c/l > 1 - D_s/\bar{D}$ ) by

$$D_c = \frac{l_c \bar{D} D_s}{l D_s - l_s \bar{D}} \quad (11)$$

### 3.3. Step three: permeation from the coating layer to the substrate

This consists of conducting a double-potentiostatic hydrogen permeation test with the coated sheet sample with thickness  $l$  now positioned in such a way that its coated surface faces the hydrogen generation compartment of the double-electrolytic cell and, hence, the uncoated (substrate) surface faces the hydrogen detection compartment.

The effective hydrogen diffusion coefficient,  $\bar{D}$ , already determined in Step two (Equation 10), will be the same for this case. Furthermore, the experimentally determined steady-state effective hydrogen permeability,  $\bar{P}_{\infty cs}$ , will enable the calculation of the hydrogen solubility in the coating layer,  $S_c$ , by

$$S_c = \frac{\bar{P}_{\infty cs}}{\bar{D}} \quad (12)$$

At this point, knowing  $D_c$ ,  $S_c$  and  $l_c$ , it is possible to determine the intrinsic hydrogen permeability of the coating layer,  $P_{\infty c}$ , by

$$P_{\infty c} = D_c S_c \quad (13)$$

By properly following these three steps of tests and analysing the combined data, one may then obtain a variety of hydrogen permeation parameters for the substrate, coating layer and the composite material, such as  $P_{\infty s}$ ,  $D_s$ ,  $S_s$ ,  $P_{\infty c}$ ,  $D_c$ ,  $S_c$ ,  $\bar{P}_{\infty sc}$ ,  $\bar{P}_{\infty cs}$  and  $\bar{D}$ .

### 3.4. Designing layers for hydrogen interaction

With the use of the above methodology one may design layers fitted to the desired purpose with respect to the interaction with hydrogen. To fulfil this objective it is necessary to define the type of layer (composition, structure, microstructure) and to find the thickness that will furnish the feature of interest. This may be a barrier or enhancer of either hydrogen entry into or exit from the composite material.

#### 3.4.1. Conditions for blocking or enhancing the ingress of hydrogen into layered materials

In this situation one considers the existence of a coating layer on the surface of hydrogen entry into the material. Taking  $\beta = l_c/l$ , Equation 8 may be rewritten for a single coating layer as

$$\bar{D} = 1 / \left( \frac{1 - \beta}{D_s} + \frac{\beta}{D_c} \right) \quad (14)$$

From Equations 12 and 14 one may express the overall steady-state hydrogen permeability in the composite material, by permeating from the coating layer to the substrate, by

$$\bar{P}_{\infty cs} = S_c / \left( \frac{1 - \beta}{D_s} + \frac{\beta}{D_c} \right) \quad (15)$$

A coating layer will play the role of an efficient barrier for hydrogen entry into the material if  $\bar{P}_{\infty cs} \ll P_{\infty s}$  holds true. On the other hand, the ingress of hydrogen into the material will be enhanced if  $\bar{P}_{\infty cs} \gg P_{\infty s}$ . Because the solubilities and diffusivities of hydrogen in the substrate and in the coating layer are intrinsic properties of these materials at constant temperature and for a given choice of materials, the possibility of a coating layer acting as a barrier for hydrogen entry into the material or yet favouring this process, as mentioned above, will depend essentially on the thickness of the layer. Furthermore, a critical value of  $\beta$  (termed  $\beta_c$ ), for which

$$\bar{P}_{\infty cs} = P_{\infty s} \quad (16)$$

may be expressed, by substituting Equations 9, 12 and 14 into Equation 16, as

$$\beta_c = \frac{(S_c/S_s) - 1}{(D_s/D_c) - 1} \quad (17)$$

Fig. 1 shows the behaviour of  $\beta_c$  as a function of the intrinsic diffusivities and solubilities of hydrogen in the substrate and in the layer. Each curve in Fig. 1 represents the locii of the points for which Equation 16 holds true. Any value of the thickness of the coating layer for which the corresponding  $\beta$  is greater than the  $\beta_c$  value found for a given pair of parameters  $D_s/D_c$  and  $S_c/S_s$  in Fig. 1, will result in a reduced hydrogen permeability in the composite material as compared to that for the substrate. That is, the coating layer will be acting as a barrier for hydrogen ingress into the material. The intensity of this effect will increase with increasing thickness of the layer with respect to that for which  $\beta_c$  was obtained. By analogy,  $l_c$  values giving  $\beta$  smaller than  $\beta_c$  will enhance the ingress of hydrogen into the material.

When the coating layer faces the hydrogen generation compartment of the electrochemical cell and its thickness is so small that the influence of a conceivably small hydrogen diffusion coefficient,  $D_c$ , is reduced, its hydrogen solubility will control the hydrogen permeation kinetics in the composite material. If the hydrogen solubility in the coating layer significantly exceeds that in the substrate, that is, if  $S_c \gg S_s$ , the overall steady-state hydrogen permeability in the composite material may be increased with respect to that of the substrate. Conversely, by increasing the thickness of the coating layer, a decrease of the effective hydrogen diffusion coefficient,  $\bar{D}$ , will be observed, being progressively more influenced by a small intrinsic hydrogen diffusion coefficient of the coating layer, as correctly expressed by Equation 14. As a result of this, the overall hydrogen permeability of the composite sample, which is directly proportional to  $\bar{D}$ , must decrease.

It should be remarked that the above mathematical development makes the assumption of the existence of a very steep hydrogen concentration gradient (the maximum) from the ingress to the egress surfaces of the sample. It is assumed to vary from the limit of hydrogen solubility to a null concentration. This is the condition for the greatest driving force for hydrogen permeation, maximizing the expected flux of hydrogen through the material. This means that a coating layer

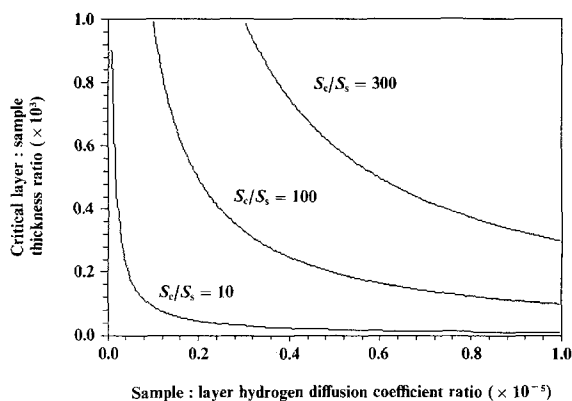


Figure 1 Critical layer to sample thickness ratio as a function of sample to layer hydrogen diffusion coefficient ratio for different types of hypothetical layers and substrates, as defined by their intrinsic hydrogen solubilities. Curves were obtained by computer simulation using Equation 17.

found to be effective as barrier for hydrogen ingress into a material by using the methodology shown herein will be still more efficient in engineering applications for which such a steep hydrogen concentration is not usually found. Hence, the present methodology gives a conservative prediction for the role of a coating layer designed to act as a barrier for hydrogen ingress into the material.

### 3.4.2. Conditions for blocking or enhancing the egress of hydrogen from layered materials

In this case we consider a single-layered material coated on the hydrogen egress surface. The effective hydrogen diffusion coefficient,  $\bar{D}$ , will be the same as that already described in Section 3.4.1, when the coating layer faced the hydrogen entry surface of the sample, for the same coating type and thickness. This is expressed in Equation 14. However, the steady-state hydrogen permeability changes to become  $\bar{P}_{\infty sc}$

$$\bar{P}_{\infty sc} = S_s \left/ \left( \frac{1 - \beta}{D_s} + \frac{\beta}{D_c} \right) \right. \quad (18)$$

Applying the same reasoning used in Section 3.4.1, from which Equation 17 arose, one verifies that the role played by the coating layer, that of rendering easier or more difficult the outgassing of hydrogen from the material, when the coating layer lies on the sample surface of hydrogen egress, is independent of the solubilities of hydrogen in the substrate or in the layer. Here, for a given thickness of coating layer, the latter will act the more efficiently as a barrier for hydrogen egress from the material the smaller is the hydrogen diffusion coefficient in the layer compared to that in the substrate. Similarly, layers for which the hydrogen diffusion coefficient is greater than found for the substrate will enhance the outgassing of hydrogen from the composite material.

## 4. Use of the proposed methodology for the determination of hydrogen permeation parameters in nitrogen ion-implanted extra-low carbon steel

Brass *et al.* [7] have recently presented a set of results for the hydrogen permeation in extra-low carbon steel sheet specimens coated on one side by nitrogen-ion implantation. Table I reproduces their Table II, with the implantation conditions and coating layer features. The unimplanted and nitrogen implanted samples were used by Brass *et al.* [7] for performing double-potentiostatic hydrogen permeation tests at 25 °C in 0.1 N NaOH. For each of the nitrogen implantation conditions results were reported for hydrogen permeation tests carried out both with the implanted surface facing the hydrogen generation compartment of the electrochemical cell as well as its hydrogen detection compartment. This permitted the application of the present methodology and thereby determination of the hydrogen permeation parameters of the coating layers and of the composite materials, as presented in Table II.

TABLE I Implantation conditions and coating layer characteristics for nitrogen ion-implanted extra-low carbon steel (after Brass *et al.* [7])

Specimen	Nominal dose ( $10^{15} \text{ cm}^{-2}$ )	Atoms dosed ( $10^{15} \text{ cm}^{-2}$ )			Film thickness (nm)
		N	O	C	
Unimplanted steel	–	20	30	15	–
Fe-10% N film	165	200	30	20	120
Fe-33% N film	400	365	40	20	100

TABLE II Hydrogen permeation data for unimplanted and nitrogen ion-implanted extra-low carbon steel

	Unimplanted steel	10% N implanted		33% N implanted	
		Steel	Coating layer	Steel	Coating layer
Intrinsic hydrogen diff. coef., $D$ ( $\text{m}^2 \text{ s}^{-1}$ )	$2.0 \times 10^{-10a}$	–	$2.5 \times 10^{-15}$	–	$4.7 \times 10^{-16}$
Effective hydrogen diff. coef., $\bar{D}$ ( $\text{m}^2 \text{ s}^{-1}$ )	–	$1.9 \times 10^{-11}$	–	$4.6 \times 10^{-12}$	–
Hydrogen solubility ( $10^3 \text{ m}^3 \text{ H}_2 / \text{m}^3$ )	4.5 <sup>a</sup>	–	39.2	–	71.1
Steady-state hydrogen permeability ( $\text{m}^3 \text{ H}_2 \text{ m m}^{-2} \text{ s}^{-1}$ )	$\bar{P}_{\infty s}^a$ $9.0 \times 10^{-13}$	$\bar{P}_{\infty sc}^a$ $0.9 \times 10^{-13}$ $\bar{P}_{\infty cs}^a$ $7.5 \times 10^{-13}$	$P_{\infty c}$ $9.0 \times 10^{-17}$	$\bar{P}_{\infty sc}^a$ $0.2 \times 10^{-13}$ $\bar{P}_{\infty cs}^a$ $3.3 \times 10^{-13}$	$P_{\infty c}$ $3.4 \times 10^{-17}$

<sup>a</sup> Experimental data from Brass *et al.* [7].

Data in Table II shows that nitrogen-ion implantation on extra-low carbon steel gives rise to a surface layer where the mobility of hydrogen is greatly reduced by comparison to that in the unimplanted material, as depicted by a very low hydrogen diffusion coefficient. Conversely, the solubility of hydrogen is increased in such layers. Both effects are more pronounced the greater is the ion implantation dose used, and hence the greater the nitrogen concentration in the implanted layer. Although not as much as for the coating layers themselves, the hydrogen diffusivity of the composite materials,  $\bar{D}$ , measured at steady-state permeation, also falls off. Because the decrease in hydrogen diffusivity is much larger than the increase in hydrogen solubility in the coating layer, its hydrogen permeability is much smaller than in the composite materials or in the unimplanted steel. This is also the reason why these coatings are more effective barriers for hydrogen to diffuse out of the steel sample than to be introduced into it. In other words, the same nitrogen-implanted layer in extra-low carbon steel will play the role of a better impeding layer to block the outgassing of hydrogen from the steel sample than to avoid it entering the material.

As remarked in Sections 3.4.1 and 3.4.2, at constant layer thickness, the hydrogen diffusivity in the layer is the controlling parameter for the blockage of hydrogen outgassing from the sample, while the relative magnitudes of the intrinsic hydrogen solubilities and diffusivities of the layer and the substrate will determine the role played by the coating layer with respect to the ingress of hydrogen into the material. Fig. 2 shows a schematic representation of the expected hydrogen concentration profiles through the thickness

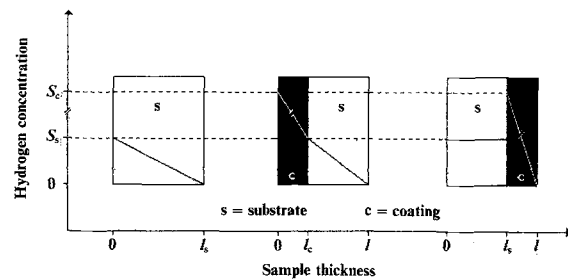


Figure 2 Schematic representation of the expected hydrogen concentration profiles in the extra-low carbon steel substrate and in the nitrogen ion-implanted layers for double-potentiostatic hydrogen permeation at steady state in nitrogen implanted steel.

of unimplanted and nitrogen ion-implanted samples used in double-potentiostatic hydrogen permeation tests at steady state. One observes the existence of steep hydrogen concentration gradients at this steady state, throughout the thickness of the substrate, both for the uncoated sample and for the composite material, provided hydrogen permeation in the composite material is performed from the layer to the substrate. However, this changes drastically, approaching a flat profile at steady state, if hydrogen permeation is carried out in the opposite sense. It stems from this fact that the chemical potential of hydrogen decreases through the sample's thickness and hence also the driving force for unidirectional hydrogen solid-state diffusion throughout the sample. This is why the overall hydrogen permeability through the composite material is so small when the coating layer faces the hydrogen egress (hydrogen detection) surface of the sample (Table II), provided that the hydrogen diffusion coefficient in the layer is smaller than in the substrate.

The effective steady-state hydrogen diffusion coefficient,  $\bar{D}$ , obtained for the composite material is independent of the way in which the hydrogen permeation test is performed, that is, it remains the same if a given implanted layer faces the hydrogen ingress or the hydrogen egress side of the sample in the electrolytic cell. However, it is very much affected by the value of  $\beta$  (the layer to sample thickness ratio) and by the nitrogen concentration in the layer, as depicted in Fig. 3. A simulation of the behaviour of the nitrogen-implanted extra-low carbon steel with respect to the hydrogen diffusivity is presented in Fig. 3 by using Equation 14. It shows that very thin layers of the type analysed here, are able to induce a steep drop in the effective hydrogen diffusion coefficient of the nitrogen ion-implanted steel.

Additional simulations, presented in Fig. 4, were undertaken for the overall hydrogen permeabilities through the coated steel, using Equations 15 and 18, for the steady-state hydrogen permeation being performed in the senses coating layer-substrate and substrate-coating layer, respectively. Again, it may be remarked that fairly thin layers obtained by nitrogen ion implantation on extra-low carbon steel induce important reductions on the kinetics of hydrogen permeation through this composite material, as compared to the behaviour presented by the substrate steel.

## 5. Conclusions

The new methodology for interpreting electrochemical hydrogen permeation tests and their resulting data presented here, makes it possible to obtain all permeation parameters, such as steady-state hydrogen permeability, solubility and diffusivity for layered materials as well as for the coating layers themselves. For a given single-layered material with known layer thickness, three hydrogen permeation tests must be performed (one for the substrate, one permeating from the substrate to the coating, and another permeating from the coating to the substrate) to be able to determine all permeation parameters. By doing so, one may generate graphs which enable the design of layered materials of the type tested for an ample range of layer-to-sample thickness ratios, predicting the behaviour expected for the composite material with respect to the overall steady-state hydrogen permeability. It then becomes possible to design coating layers to play the role of either barriers or enhancers of hydrogen ingress into or egress from the composite material, fitting them to the desired purpose of use.

The present methodology was applied to published results of hydrogen permeation in nitrogen ion-implanted extra-low carbon steel. It was found that the hydrogen diffusivity in the nitrogen ion-implanted layer is several orders of magnitude lower than that in the substrate and that the hydrogen solubility is about one to two orders of magnitude higher. Both effects are more pronounced the greater the implantation dose used, hence, the greater the nitrogen concentration in the layer. Owing to the very small hydrogen diffusivity in such coatings, the nitrogen-ion im-

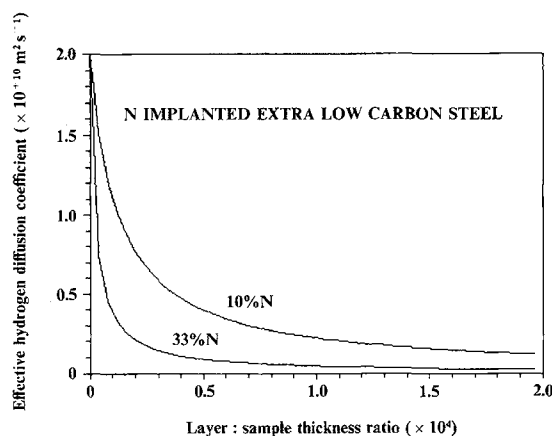


Figure 3 Effective hydrogen diffusion coefficient,  $\bar{D}$ , as a function of layer to sample thickness ratio for nitrogen ion implanted extra-low carbon steel. Simulation was performed via Equation 14 by using diffusivity of the substrate taken from the experimental data of Brass *et al.* [7] and that of the coating layer determined therefrom.

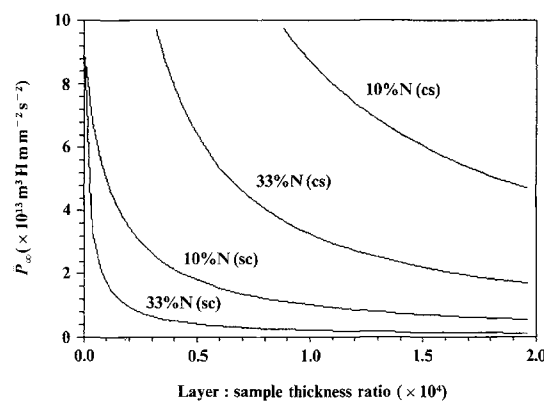


Figure 4 Steady-state hydrogen permeabilities as a function of layer to sample thickness ratio for nitrogen ion-implanted extra-low carbon steel. Simulation was performed via Equation 15 for  $\bar{P}_{\infty, cs}$  and via Equation 18 for  $\bar{P}_{\infty, sc}$  by using substrate diffusivity and solubility taken from the experimental data of Brass *et al.* [7], and coating layer diffusivity and solubility determined therefrom. cs, hydrogen permeation performed from the coating layer to the substrate; sc, the opposite case.

planted layers on extra-low carbon steel are even more efficient as impeding layers to the egress of hydrogen from the material than to block its entry. Mathematical simulation using the calculated parameters showed that very thin layers of this type (of several thousandths of a per cent of the sample's thickness) are sufficient to impose drastic changes on the steady-state hydrogen permeability through the material.

## Acknowledgements

The authors acknowledge the financial support for this research given by CNPq (grant 403188/90-3) and SCT-PR, as well as CAPES for the scholarship to F.D.F. We also thank A. H. Bott for reviewing the manuscript.

## References

1. M. A. V. DEVANATHAN and Z. STACHURSKI, *J. Electrochem. Soc.* **111** (1964) 619.
2. N. BOES and H. ZÜCHNER, *J. Less. Common Metals* **49** (1976) 223.
3. R. KIRCHHEIM and R. B. McCLELLAN, *J. Electrochem. Soc.* **127** (1980) 2419.
4. M. F. STEVENS and I. M. BERNSTEIN, *Met. Trans.* **20A** (1989) 909.
5. R. KIRCHHEIM, T. MUTSCHELE, W. KIENINGER, H. GLEITER, R. BIRINGER and T. D. KOBLE, *Mater. Sci. Engng* **99** (1988) 457.
6. J. CRANK, "Mathematics of Diffusion" (Clarendon, Oxford, 1956).
7. A. M. BRASS, J. CHENE and J. C. PIVIN, *J. Mater. Sci.* **24** (1989) 1963.

*Received 2 September  
and accepted 17 November 1992*